

---

---

# Princeton Plasma Physics Laboratory

---

---

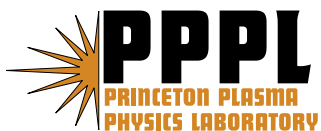
PPPL-4127

PPPL-4127

## Onset and Saturation of Ion Heating by Odd-parity Rotating-magnetic-fields in a Field-reversed Configuration

A.S. Landsman, S.A. Cohen, and A.H. Glasser

November 2005



Prepared for the U.S. Department of Energy under Contract DE-AC02-76CH03073.

# **Princeton Plasma Physics Laboratory**

## **Report Disclaimers**

---

### **Full Legal Disclaimer**

This report was prepared as an account of work sponsored by an agency of the United States Government. Neither the United States Government nor any agency thereof, nor any of their employees, nor any of their contractors, subcontractors or their employees, makes any warranty, express or implied, or assumes any legal liability or responsibility for the accuracy, completeness, or any third party's use or the results of such use of any information, apparatus, product, or process disclosed, or represents that its use would not infringe privately owned rights. Reference herein to any specific commercial product, process, or service by trade name, trademark, manufacturer, or otherwise, does not necessarily constitute or imply its endorsement, recommendation, or favoring by the United States Government or any agency thereof or its contractors or subcontractors. The views and opinions of authors expressed herein do not necessarily state or reflect those of the United States Government or any agency thereof.

### **Trademark Disclaimer**

Reference herein to any specific commercial product, process, or service by trade name, trademark, manufacturer, or otherwise, does not necessarily constitute or imply its endorsement, recommendation, or favoring by the United States Government or any agency thereof or its contractors or subcontractors.

## **PPPL Report Availability**

---

### **Princeton Plasma Physics Laboratory**

This report is posted on the U.S. Department of Energy's Princeton Plasma Physics Laboratory Publications and Reports web site in Fiscal Year 2006.

The home page for PPPL Reports and Publications is:

[http://www.pppl.gov/pub\\_report/](http://www.pppl.gov/pub_report/)

### **Office of Scientific and Technical Information (OSTI):**

Available electronically at: <http://www.osti.gov/bridge>.

Available for a processing fee to U.S. Department of Energy and its contractors, in paper from:

U.S. Department of Energy  
Office of Scientific and Technical Information  
P.O. Box 62  
Oak Ridge, TN 37831-0062

Telephone: (865) 576-8401

Fax: (865) 576-5728

E-mail: [reports@adonis.osti.gov](mailto:reports@adonis.osti.gov)

# Onset and saturation of ion heating by odd-parity rotating-magnetic-fields in a field-reversed configuration

A.S. Landsman<sup>a</sup>, S.A. Cohen<sup>b</sup>, A.H. Glasser<sup>c</sup>

October 24, 2005

## Abstract

Heating of figure-8 ions by odd-parity rotating magnetic fields ( $RMF_o$ ) applied to an elongated field-reversed configuration (FRC) is investigated. The largest energy gain occurs at resonances ( $s \equiv \omega_R/\omega$ ) of the  $RMF_o$  frequency,  $\omega_R$ , with the figure-8 orbital frequency,  $\omega$ , and is proportional to  $s^2$  for  $s$  – even resonances and to  $s$  for  $s$  – odd resonances. The threshold for the transition from regular to stochastic orbits explains both the onset and saturation of heating. The FRC magnetic geometry lowers the threshold for heating below that in the tokamak by an order of magnitude.

Heating, *i.e.*, stochastic energy gain, of charged particles by time-varying fields is a complex and fundamental phenomenon critically important to as diverse areas of plasma physics as fusion research[1] and plasma processing[2]. Well known are the effects of simple resonances and particle collisionality on the heating of magnetized plasmas. Far less well explored is the role of an inhomogeneous static magnetic-field geometry. Because of its relevance to space plasmas[3], plasma processing[4], and magnetic-confinement controlled-fusion research[5], the field-reversed configuration (FRC, see Fig. 1) – with its poloidal field nulls, lack of toroidal field, and strong field gradients – is an important system in which to explore the effects of magnetic field geometry on particle dynamics under the influence of time-varying fields.

Even with axial symmetry, a static FRC allows charged-particle orbits that are regular or ergodic[6, 7]. First studies of single-particle orbits in FRCs assumed time invariance and spatial symmetries that reduced the problem to one or two dimensions, allowing Kolmogorov-Arnold-Moser (KAM) surfaces to exist[8] and limiting excursions in phase space. The addition of a rotating magnetic field (RMF)[9] breaks the angular invariance of the FRC, creating a three-dimensional system without bounding KAM surfaces and opening the possibility for large excursions in phase space and energy. These excursions can have beneficial results, such as ion heating[10, 11], or detrimental ones, such as loss of confinement. In this paper we present studies of ion orbits in FRCs with RMF applied: the goal is to understand the threshold for chaos and the role of resonances in the non-linear growth and subsequent saturation of ion energy. We restrict attention to the novel odd-parity RMFs ( $RMF_o$ ) because of field closure[12] and encouraging recent experimental

results[13]. We show that the same mechanism is responsible for the initial ion heating and its ultimate saturation.

Studies of stochastic ion heating by perpendicularly propagating electrostatic waves in tokamaks were performed with similar Hamiltonian techniques and research goals [14, 15]. The results we report are markedly different because of fundamental differences in the magnetic field geometry of the two devices.

Earlier papers [10, 11], which used the RMF numerical code to investigate  $RMF_o$ s applied to FRCs, showed that the relevant frequency range for ion heating was broad,  $|\Omega| \sim 0.2 - 2$ , where  $\Omega \equiv \omega_R/\omega_{ci}$ ,  $\omega_R$  is the  $RMF_o$  frequency,  $\omega_{ci} = qB_a/mc$  is the ion-cyclotron frequency in the axial field at the FRC's center,  $B_a$ ,  $m$  is the ion mass, and  $q$  is the ion charge. These papers reported significant ion heating even for low relative RMF amplitude,  $B_R$ :  $B_R/B_a \sim 5 \times 10^{-4}$ . Phase de-coherence of ion orbits, with respect to the periodic electric fields created by the  $RMF_o$ , is a necessary condition for ion heating. Strong gradients and regions of field reversal in the FRC provide locations for possible phase de-coherence. For a 10-cm FRC having an ion density of  $10^{14} \text{ cm}^{-3}$  and an ion energy of 100 eV, Coulomb collisions will be  $10\times$  less frequent than the stochastic effects described herein[10].

The question arose whether, in spite of the existence of strong field gradients, ion-cyclotron resonances (ICRs) were important to ion heating. We show that ICRs are important, but with significant differences from the standard ICR picture. More rapid heating occurs at low  $B_R/B_a$  for figure-8 orbits (see Fig. 1b)) than for cyclotron orbits, though the latter have a more clearly resonant interaction with  $RMF_o$ . Figure-8 orbits cross the field-reversal and strong-gradient regions (twice) every orbit cycle, possibly losing phase coherence at each traversal. In contrast, cyclotron orbits may only incur phase de-coherence at the less frequent excursions to the axial extremes of their orbits. Betatron orbits have a less non-linear nature and hence are also less well heated than figure-8 orbits. Because figure-8 orbits are representative of a large fraction of ions in hot fusion FRC plasmas and because they represent the physically interesting situation of motion in a double potential well[16], we focus on them. The studies presented herein also clarify why high-energy orbits tend to interact regularly with  $RMF_o$ , leading, importantly, to a saturation of ion heating by  $RMF_o$  and a method for tuning ion energy.

We follow Ref. [11] by using the same equations for the  $RMF_o$  and a Solov'ev equilibrium for the FRC, with the notation, see Fig. 1a):  $R$  = FRC separatrix radius in midplane;  $Z$  = FRC axial half length;  $\kappa \equiv Z/R$ , FRC elongation;  $r$  = radial coordinate;  $z$  = axial coordinate;  $\phi$  = azimuthal coordinate;  $p_i$  = canonical momenta;  $P \equiv 2p_\phi/qB_aR^2$ , normalized  $p_\phi$ ;  $\mathbf{A}$  = vector potential of RMF and FRC;  $\psi = \phi - \omega_R t$ ;  $k = l\pi/\kappa R$  = axial wave number of the  $RMF_o$ ;  $l$  = axial mode number; and time,  $\tau$ , in units of  $2\pi/\omega_{ci}$ .

The shape of the effective potential-energy surface on which an ion moves depends on  $P$  and  $z$ [17]: figure-8 orbits may be confined to the  $z = 0$  subspace, or to a potential-well minimum above or below  $z = 0$ , or may oscillate across  $z = 0$ . Orbits confined to the  $z = 0$  subspace are amenable to an analytic analysis and are the appropriate choice to analyze because of the  $RMF_o$ 's electric fields,  $\mathcal{E}_r$  and  $\mathcal{E}_\phi$ , there. Each cross-section in  $z$  is either a double potential well, allowing both cyclotron and figure-8 orbits, or a raised potential, corresponding to betatron orbits. Cyclotron orbits feel a force towards larger  $|z|$ , thus eventually enter a region where the barrier between the

double wells is low enough for them to traverse, thereby becoming figure-8 orbits. Since cyclotron orbits interact regularly with RMF, except at these axial extremes, their random fluctuations in energy appear less frequently than for orbits which are always figure-8. Moreover, figure-8 orbits have greater radial excursions, hence gain more energy from the radial electric field of the  $RMF_0$ . It follows that the heating of figure-8 orbits is an upper limit for the heating of all ions in the FRC and that the threshold for heating is highest in the  $z = 0$  subspace. Extensive numerical simulations, performed with the  $RMF$  code, confirmed this.

We first examined whether the broad  $\Omega$  range for heating is due to resonances at the fundamental ICR frequency. As described below, the answer is no. Instead high-harmonic resonances occur because the frequency of the figure-8 orbit is highly nonlinear. (High-harmonic resonances have recently been observed in an RMF experiment[18].) As the energy of a figure-8 orbit decreases, the ratio  $s \equiv \omega_R/\omega$  increases because the ion's frequency,  $\omega$ , slows down as it gets closer to the phase-space separatrix created by the hump in the double potential well. A set of resonances with the  $RMF_0$  occurs at integral values of  $s$ .

Figure 2a) shows the  $RMF$ -code-calculated time dependence of ion energy for two values of  $B_R$  for a 1-keV ion initiated in a figure-8 orbit with zero axial velocity in the  $z = 0$  subspace of an FRC having  $R = 10$  cm,  $\kappa = 5$ ,  $\Omega = 0.9$ , and  $B_a = 20$  kG. Regular motion, with a clear  $s = 5$  component, is seen for  $B_R = 2$  G. The energy fluctuations are small ( $\sim 15\%$ ) for  $B_R = 2$  G and large,  $> 100\%$ , for  $B_R = 20$  G. For  $B_R = 2$  G, the fast Fourier transform (FFT) of ion energy, Figure 2 b), shows sharp peaks in frequency space, indicative of regular motion. The separation between peaks,  $\Delta f$ , is  $0.207 \pm 0.002$ , in units of  $\omega_{ci}$ . For  $B_R = 20$  G, the FFT shows broadband noise at a  $30\times$  higher absolute level. Under these conditions, betatron (also shown in Fig. 2b)) and cyclotron orbits (not shown) display regular motion — sharp peaks in their FFTs — with energy fluctuations less than 7%, even for  $B_R = 20$  G. Figure 2c) shows  $\Delta f$  vs  $\tilde{E}$ , initial energy normalized to  $E_n \equiv q^2 B_a^2 R^2 / 2m$ , for three values of initial  $P$  and low  $B_R$ . Below  $P = 0.25$  orbits may be cyclotron or figure-8; above  $P = 0.25$  orbits are betatron. A logarithmic drop in  $\Delta f$  is seen for  $P = 0.1$  and  $0.2$  at an energy corresponding to the phase-space separatrix energy, at the transition of cyclotron into figure-8 orbits. Little change in  $\Delta f$  occurs for betatron orbits.

In heating, the variance of energy, and therefore the maximum energy,  $E_{max}$ , will increase with time[19]. Figure 3a) shows  $E_{max}$  attained by an initially figure-8 orbit as a function of time for four  $B_R$  values and the same FRC parameters as in Fig. 2.  $E_{max}$  displays saturation behavior quickly, implying phase coherence growing with increasing energy. The threshold for heating is at  $B_R \sim 3$  G, above which  $E_{max}$  grows  $\propto B_R^{1.5}$ . Figure 3b) compares  $E_{max}$  vs  $B_R$  for figure-8 ( $P = 0.22$ ), betatron ( $P = 0.26$ ), and cyclotron ( $P = 0.19$ ) orbits initiated in the  $z = 0$  subspace at the same radial position,  $r/R = 0.8131$ , and the same energy, 1000 eV, for a simulation time of  $\tau = 10^4$ . Heating of figure-8 orbits occurs at lower  $B_R$  than for cyclotron or betatron orbits. At  $B_R \sim 20$  G, FFTs of energy for figure-8 ions initiated at higher energy,  $E > 0.03E_n \sim 30$  keV, in the  $z = 0$  subspace show sharp peaks and little further gain in energy. The regular interaction with  $RMF_0$  of these higher energy figure-8 orbits may be understood by the greater separation between resonances in phase-space[7, 20] with increasing energy (or  $\omega$ ).

We have calculated the  $RMF_0$ -induced energy gain of a figure-8 orbit in a single half period of its motion as a first-order correction to the one-dimensional motion along  $r$ . For  $P < 0.25$ , the shape of the effective potential,  $V(r)$ , is a double well[7, 21], corresponding to cyclotron orbits

(in either well) inside the phase-space separatrix and to figure-8 orbits (moving across both wells) outside the phase-space separatrix. The figure-8 orbit is approximated by motion in a symmetric double well:  $\rho \equiv \frac{r}{R} = \rho_0 + a_1 \cos[\omega(t - t_0)] + a_2 \cos[3\omega(t - t_0)]$ , with  $a_1/a_2 \sim 10$ . The amplitudes of oscillation,  $a_1$  and  $a_2$ , are determined by the total energy. The energy change from the interaction with the field is given by  $dH/dt = q\vec{\mathcal{E}} \cdot \vec{v} = q(\mathcal{E}_r v_r + \mathcal{E}_\phi v_\phi)$ , with  $c\vec{\mathcal{E}} = -\partial\vec{A}/\partial t$ . After some algebra and integrating over a single half oscillation [20, 22], we get the energy gain from the interaction with the  $\mathcal{E}_r$  and  $\mathcal{E}_\phi$  components of the RMF. The biggest energy change occurs for a resonance between the  $RMF_o$  and the Fourier components of the orbital motion, *i.e.*,  $\omega_R/\omega = s$ , where  $s$  is an integer. The  $\mathcal{E}_r$ - and  $\mathcal{E}_\phi$ -induced radial and azimuthal portions of the energy change ( $\Delta E$ ) in a single half oscillation for an  $s$  resonance are:

$$\Delta E_r = H_0 \left( \sum_{n=1}^{9, n \neq s} F_n(\omega) \cos(\Psi_0) + [\hat{F}_0 + F_s] \sin(\Psi_0) \right) \quad (1)$$

$$\Delta E_\phi = H_0 \left( \sum_{n=0}^{8, n \neq s} Q_n(\omega) \cos(\Psi_0) + Q_s(\omega) \sin(\Psi_0) \right) \quad (2)$$

where  $F_n(\omega) = C_n [(-1)^{s+n} - 1] \frac{n}{s^2 - n^2}$ ,  $\hat{F}_0 = -\frac{C_0}{s} ((-1)^s - 1)$ ,  $F_s = \frac{\pi}{2} C_s$ ,  $Q_s(\omega) = \frac{\pi}{2} \left( \frac{\omega_{ci}}{\omega} \right) K_s$ ,  $Q_n(\omega) = K_n [(-1)^{s+n} - 1] \frac{s}{s^2 - n^2} \frac{\omega_{ci}}{\omega}$ ,  $\Psi_0 = \phi - \omega_R t_0$ ,  $t_0$  is the initial time,  $H_0 = mkR^3 \omega_{ci} \omega_R B_R / 2B_a$ , and the  $C_n$  depend on  $\rho_0$ ,  $a_1$  and  $a_2$ . Since the total energy is  $H \sim \frac{1}{2} m(R\omega a_1)^2$  and  $|\Omega| \sim 1$ , the relative fluctuations in energy during an oscillation are of order,  $\max \Delta E_{\text{odd}}/H \sim O(10^2 s B_R/B_a)$ , and  $\max \Delta E_{\text{even}}/H \sim O(10 s^2 B_R/B_a)$ . These predict significant energy gain for figure-8 orbits over a single oscillation, even for a relatively low amplitude RMF,  $B_R/B_a \sim 10^{-3}$ . The energy gain for  $s$  - *even* resonances has an  $s^2$  dependence while  $s$  - *odd* energy gain has a linear dependence on  $s$ . Resonances with an odd value of  $s$  show better heating than  $s$  - *even* resonances, especially at lower values of  $s$ , where the ion energy is higher. Thus, the heating observed for figure-8 orbits at higher energies results primarily from an overlap of odd- $s$  resonances.

Using the condition for exponential separation of trajectories[22], we now determine the threshold for the ergodicity of ion trajectories, essential to convert energy gain to stochastic heating. The change in energy over an oscillation is used to map the dynamics:  $E_{j+1} = E_j + \Delta E(t_j)$ ;  $t_{j+1} = t_j + \frac{\pi}{\omega(E_{j+1})}$  where  $t_j$  is the time of the start of successive ion oscillations at  $\rho = \rho_{\text{max}} \equiv \rho_0 + a_1$  and  $\Delta E(t_j)$  is  $\Delta E_r(t_j) + \Delta E_\phi(t_j)$ , with the substitutions  $\Psi \rightarrow \Psi_j$ ,  $\Psi_j = \phi - \omega_R t_j$ , and  $\Delta E \rightarrow \Delta E(t_j)$ . The dynamics will be chaotic if exponential separation of trajectories, *i.e.*,  $K > 1$ , occurs, where  $K = \max \left| \frac{dt_{j+1}}{dt_j} - 1 \right|$ . In dimensionless variables,  $\tilde{E} = (m/b^2 R^2) E$  and  $\tilde{\omega} = m\omega/b = 2\omega/\omega_{ci}$ , where  $b = qB_a/2c$ .  $K$  for odd and even resonances are:

$$K_{\text{odd}} \approx 8\pi s \left( \frac{1}{kR} \right) \left( \frac{B_R}{B_a} \right) \frac{d\tilde{\omega}(\tilde{E})}{d\tilde{E}} \quad (3)$$

$$K_{\text{even}} \approx \frac{\pi}{2} s^2 (kR) \left( \frac{B_R}{B_a} \right) \frac{d\tilde{\omega}(\tilde{E})}{d\tilde{E}} \quad (4)$$

Based on these, increasing the axial wavenumber,  $k$ , of the  $RMF_o$  should lower the chaos threshold for  $s$  - *odd* resonances while raising the threshold for  $s$  - *even* resonances. This is borne out by numerical simulation.

Fig. 3c) shows  $d\tilde{\omega}(\tilde{E})/d\tilde{E}$  vs.  $\tilde{E}$  for figure-8 orbits having  $P = 0.15$ . At energies very close to the separatrix,  $d\tilde{\omega}(\tilde{E})/d\tilde{E}$  grows as  $(\tilde{E} - \tilde{E}_h)^{-5/6}$ , where  $\tilde{E}_h$  is the energy at the phase-space

separatrix. The large growth of  $d\tilde{\omega}(\tilde{E})/d\tilde{E}$  near the separatrix corresponds to a large increase in non-linearity of the figure-8 orbital frequency.

The greatest rate of stochastic heating is expected to occur for lower energy figure-8 orbits where the values of  $s$  and  $d\tilde{\omega}(\tilde{E})/d\tilde{E}$  are higher. As  $B_R$  is increased, the stochastic region above the phase-space separatrix will broaden. Close to the separatrix, even very low amplitudes of  $B_R$  should produce chaotic orbits. Eqns. 3) and 4), combined with Fig. 3c), can be used to estimate the relative amplitude of  $B_R$  needed to produce stochasticity and heating. For example,  $s = 3$  resonance occurs at  $\tilde{E} \approx .0185$ , corresponding to  $d\tilde{\omega}(\tilde{E})/d\tilde{E} \approx 25$ , see Fig. 3c). Using Eqn. 3) and  $kR \sim 1$ , chaotic trajectories are to be expected for all  $s - odd$  resonances with  $s \geq 3$  and  $B_R/B_a \geq 5 \cdot 10^{-4}$ , for  $\Omega \sim 1$ , the assumption used in the derivation. These findings approximately agree with the numerical findings. Changing the value of a  $P$  changes the scale of  $\tilde{E}$ , but does not have a substantial effect on the value of  $d\tilde{\omega}(\tilde{E})/d\tilde{E}$  at different resonances. Thus  $P$  determines the energy range over which figure-8 orbits get heated, with greater energy range for lower values of  $P$ , while not affecting the approximate structure of phase space. In Fig. 3c), all  $s > 4$  resonances are located to the left of  $\tilde{E} \approx 0.013$ , hence occur over the interval  $\delta\tilde{E} \sim 0.003$ . This leads to much greater chaos closer to the phase-space separatrix where the closely spaced resonances overlap. Thus, lower-energy figure-8 orbits are more chaotic and much better heated by the  $RMF_o$  than the higher energy ones. Fig. 3d) shows this effect for two values of  $P$ : 0.17 and 0.2. Figure-8 orbits are not further heated once their energy reaches (or initially exceeds) the curved line appropriate for each  $P$  value. The simplifications on which Eqns. 3) and 4) are based become less accurate at  $B_R/B_a > 0.001$ .

Among the clearest differences between these results for the FRC and those reported for the tokamak[15] are: 1) The non-linearities for the FRC arise from the double potential well and field gradient and their direct effects on the particle orbit. Those in the tokamak arise from trapping in the wave field – hence require a stronger wave field – and resonance between the cyclotron motion and the wave field, resulting in a single large resonance and large first-order islands. In contrast, close spacing in phase space between resonances of a figure-8 orbit leads to an overlap between resonances and the observed stochastic heating for figure-8 orbits in FRCs. The importance of the time-varying field,  $\mathcal{E}$ , in the tokamak analysis is to create a small nonlinearity in this 2-D system (of the order of  $\mathcal{E}/B$ ) which leads to resonances between the two degrees-of-freedom, not between the  $\mathcal{E}$  field and the ion trajectory. 2) In the tokamak, heating occurs at  $10\times$  higher values of  $\Omega$  (over 20 vs 1 in the FRC) and lower values of  $\omega_R/kv_{i,thermal}$  ( $\sim 1$  vs 10). 3) The threshold for heating in the FRC is lower by the factor  $sd\tilde{\omega}(\tilde{E})/d\tilde{E}$ , through which the effect of the FRC's double effective-potential well is clear.

In summary, the energy gain in an orbital period due to  $RMF_o$  was calculated for a figure-8 orbit in an FRC. Resonances of  $\omega_R$  with  $\omega$  produce significant energy gain. Odd- $s$  resonances more effectively heat for high energy (lower  $s$ ) figure-8 orbits. The energy gain in a oscillation was used to map the dynamics and a criterion for the exponential separation of trajectories was used to find the threshold for chaotic orbits.  $K$ , the measure of the rate of trajectory separation, increases with  $B_R$ . At higher energies, the orbits are less chaotic due to both a lower value of  $s$  and, more importantly, to a decreased nonlinearity reducing  $d\tilde{\omega}(\tilde{E})/d\tilde{E}$ .

This work was supported, in part, by the U.S. Department of Energy Contract No. DE-AC02-76-CHO-3073. We thank C.K. Phillips for helpful comments.

<sup>a</sup> Naval Research Laboratory, Washington, DC (e-mail: alandsma@cantor.nrl.navy.mil)

<sup>b</sup> Princeton Plasma Physics Laboratory, Princeton University, Princeton, NJ (e-mail: scohen@pppl.gov)

<sup>c</sup> Los Alamos National Laboratory, Los Alamos, NM (e-mail: ahg@lanl.gov)

## References

- [1] T.H. Stix. *Waves in Plasmas*. American Institute of Physics, New York, 1992.
- [2] M. A. Lieberman and A. J. Lichtenberg. *Principles of Plasma Discharges and Materials Processing*. John Wiley and Sons, Inc., New York, 1994.
- [3] J. Chen. Nonlinear dynamics of charged particles in the magnetotail. *J. Geophys. Res.*, 97:15011, 1992.
- [4] I. Yu. Kostukov and J.M. Rax. Stochastic heating in field-reversed low pressure discharges. *Phys. Plasmas*, 7:185, 2000.
- [5] M. Tuszewski. Review paper: Field reversed configurations. *Nucl. Fusion*, 28:2033–92, 1988.
- [6] J. M. Finn and R. N. Sudan. Review paper: Field reversed configurations with a component of energetic particles. *Nucl. Fusion*, 22:1443–1518, 1982.
- [7] A. S. Landsman, S. A. Cohen, M. Edelman, and G. M. Zaslavsky. Nonlinear resonance and chaotic trajectories in magnetic field-reversed configuration. *Communications in Nonlinear Science and Numerical Simulations*, 10:617, 2005.
- [8] A. J. Lichtenberg and M. A. Lieberman. *Regular and Chaotic Dynamics*. Springer-Verlag, New York, 1992.
- [9] W. N. Hugrass and M. Turley. The orbits of electrons and ions in the fields of the rotamak. *J. Plasma Phys.*, 37:1–13, 1987.
- [10] S. A. Cohen and A. H. Glasser. Ion heating in the field-reversed configuration by rotating magnetic fields near the ion-cyclotron resonance. *Phys. Rev. Lett.*, 85:5114, 2000.
- [11] A. H. Glasser and S. A. Cohen. Ion and electron acceleration in the field-reversed configuration with odd-parity rotating magnetic field. *Phys. Plasmas*, 9:2093–2102, 2002.
- [12] S. A. Cohen and R. D. Milroy. Maintaining the closed magnetic-field-line topology of a field-reversed configuration with the addition of static transverse magnetic fields. *Phys. Plasmas*, 7:2539, 2000.
- [13] H.Y. Guo, A.L. Hoffman, R.D. Milroy, K. E. Miller, and G. R. Votroubek. Stabilization of interchange modes by rotating magnetic fields. *Phys. Rev. Lett.*, 94:185001, 2005.
- [14] C.F.F. Karney and A. Bers. Stochastic ion heating by a perpendicularly propagating electrostatic wave. *Phys. Rev. Lett.*, 39:550, 1977.
- [15] C.F.F. Karney. Stochastic ion heating by a lower hybrid wave. *Phys. Fluids*, 21:1584, 1978.



- [16] A. I. Neishtadt, V. V. Sidorenko, and D. V. Treschev. Stable periodic motions in the problem of passage through separatrix. *Chaos*, 7:2–11, 1997.
- [17] A. S. Landsman, S. A. Cohen, and A. H. Glasser. Regular and stochastic orbits of ions in a highly prolate field-reversed configuration. *Phys. Plasmas*, 11:947, 2004.
- [18] Fangchuan Zhong, Yuri Petrov, and Tian-Sen Huang. High harmonic fields in a rotamak plasma. *Phys. Plasmas*, 11:L1, 2004.
- [19] M. Kac. *Probability and Related Topics in Physical Sciences*. New York: Interscience, 1958.
- [20] A.S. Landsman. Single ion dynamics inside the magnetic field-reversed configuration. *PhD. Thesis, Princeton University*, 2005.
- [21] M. Y. Wang and G. H. Miley. Particle orbits in field-reversed mirrors. *Nucl. Fusion*, 19:39–49, 1979.
- [22] G. M. Zaslavsky. *Physics of chaos in Hamiltonian systems*. Imperial College Press, London, 1998.

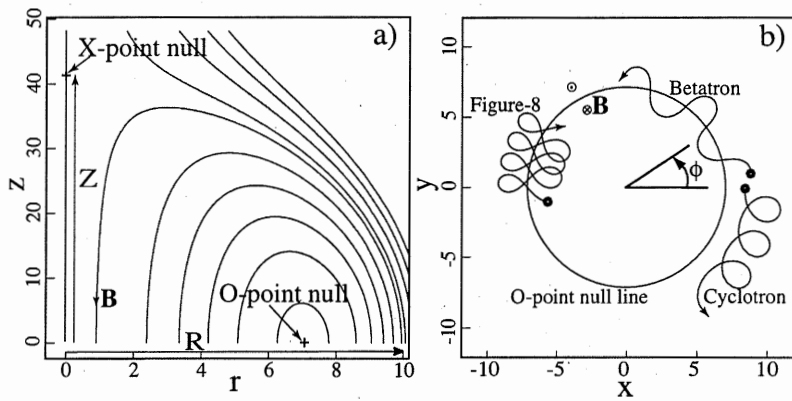


Figure 1: a) Shape of FRC magnetic field in  $z$ - $r$  plane.  $\kappa = 4.1$ . b) Shapes of typical cyclotron, betatron and figure-8 orbits in  $z = 0$  plane.

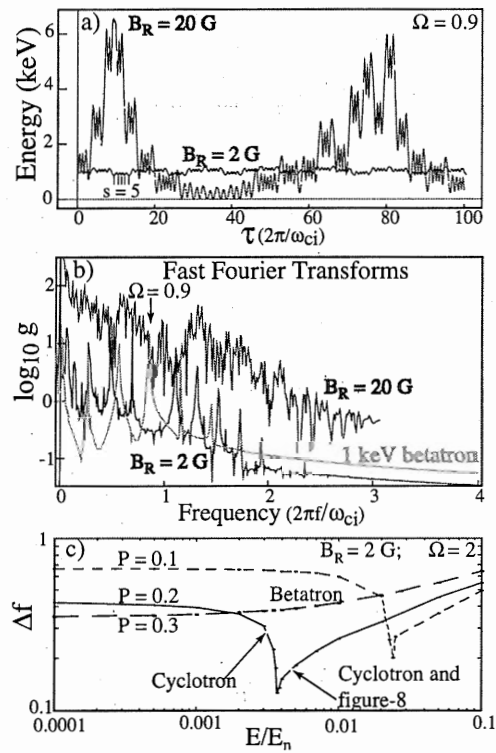


Figure 2: Results of numerical simulation of ion trajectories in an FRC with  $RMF_0$ . a) Figure-8 ion energy *versus* time for two values of  $B_R$ . b) FFTs of ion energy for the two cases shown in a) and also for a betatron orbit. c) Separation between resonances,  $\Delta f$ , *versus* normalized initial energy for  $P = 0.1, 0.2$  and  $0.3$ , at low  $B_R$ .

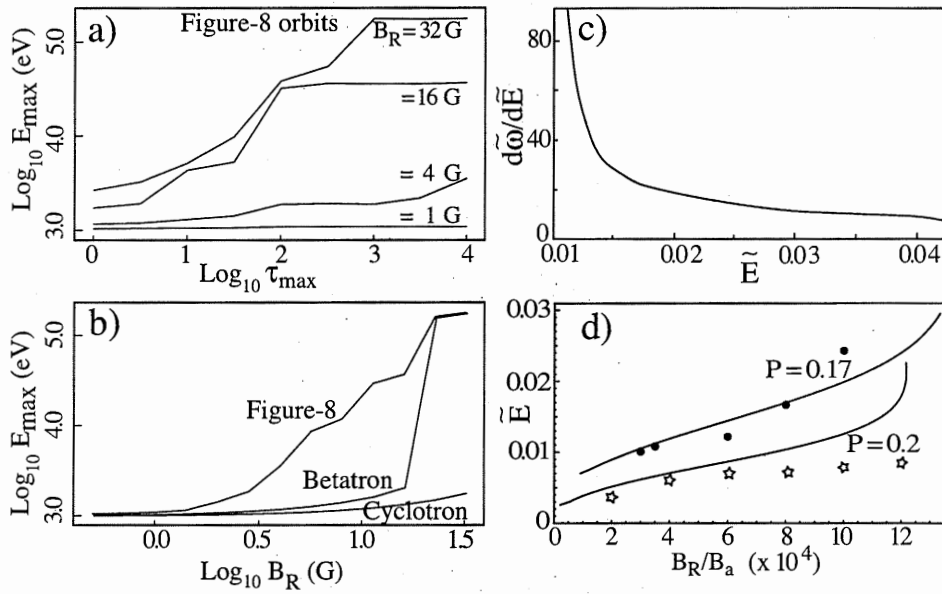


Figure 3: a) Maximum energy attained *versus* time for four values of  $B_R$ . b) Maximum energy attained by  $\tau = 10^4$  *versus*  $B_R$  by three types of orbits. c)  $d\tilde{\omega}(\tilde{E})/d\tilde{E}$  *versus*  $\tilde{E}$  for figure-8 orbits.  $P = 0.15$ . d) Curves: Threshold  $\tilde{E}$  for saturation of stochastic heating *versus*  $B_R/B_a$ , based on Eqns 3) and 4):  $P = 0.17$  (upper curve) and  $P = 0.2$  (lower curve); Data points, dots and stars, from RMF-code.

## External Distribution

Plasma Research Laboratory, Australian National University, Australia  
Professor I.R. Jones, Flinders University, Australia  
Professor João Canalle, Instituto de Fisica DEQ/IF - UERJ, Brazil  
Mr. Gerson O. Ludwig, Instituto Nacional de Pesquisas, Brazil  
Dr. P.H. Sakanaka, Instituto Fisica, Brazil  
The Librarian, Culham Science Center, England  
Mrs. S.A. Hutchinson, JET Library, England  
Professor M.N. Bussac, Ecole Polytechnique, France  
Librarian, Max-Planck-Institut für Plasmaphysik, Germany  
Jolan Moldvai, Reports Library, Hungarian Academy of Sciences, Central Research  
Institute for Physics, Hungary  
Dr. P. Kaw, Institute for Plasma Research, India  
Ms. P.J. Pathak, Librarian, Institute for Plasma Research, India  
Dr. Pandji Triadyaksa, Fakultas MIPA Universitas Diponegoro, Indonesia  
Professor Sami Cuperman, Plasma Physics Group, Tel Aviv University, Israel  
Ms. Clelia De Palo, Associazione EURATOM-ENEA, Italy  
Dr. G. Grosso, Istituto di Fisica del Plasma, Italy  
Librarian, Naka Fusion Research Establishment, JAERI, Japan  
Library, Laboratory for Complex Energy Processes, Institute for Advanced Study,  
Kyoto University, Japan  
Research Information Center, National Institute for Fusion Science, Japan  
Professor Toshitaka Idehara, Director, Research Center for Development of Far-Infrared Region,  
Fukui University, Japan  
Dr. O. Mitarai, Kyushu Tokai University, Japan  
Mr. Adefila Olumide, Ilorin, Kwara State, Nigeria  
Dr. Jiangang Li, Institute of Plasma Physics, Chinese Academy of Sciences, People's Republic of China  
Professor Yuping Huo, School of Physical Science and Technology, People's Republic of China  
Library, Academia Sinica, Institute of Plasma Physics, People's Republic of China  
Librarian, Institute of Physics, Chinese Academy of Sciences, People's Republic of China  
Dr. S. Mirnov, TRINITI, Troitsk, Russian Federation, Russia  
Dr. V.S. Strelkov, Kurchatov Institute, Russian Federation, Russia  
Kazi Firoz, UPJS, Kosice, Slovakia  
Professor Peter Lukac, Katedra Fyziky Plazmy MFF UK, Mlynska dolina F-2, Komenskeho Univerzita,  
SK-842 15 Bratislava, Slovakia  
Dr. G.S. Lee, Korea Basic Science Institute, South Korea  
Dr. Rasulkhozha S. Sharafiddinov, Theoretical Physics Division, Institute of Nuclear Physics, Uzbekistan  
Institute for Plasma Research, University of Maryland, USA  
Librarian, Fusion Energy Division, Oak Ridge National Laboratory, USA  
Librarian, Institute of Fusion Studies, University of Texas, USA  
Librarian, Magnetic Fusion Program, Lawrence Livermore National Laboratory, USA  
Library, General Atomics, USA  
Plasma Physics Group, Fusion Energy Research Program, University of California at San Diego, USA  
Plasma Physics Library, Columbia University, USA  
Alkesh Punjabi, Center for Fusion Research and Training, Hampton University, USA  
Dr. W.M. Stacey, Fusion Research Center, Georgia Institute of Technology, USA  
Director, Research Division, OFES, Washington, D.C. 20585-1290

The Princeton Plasma Physics Laboratory is operated  
by Princeton University under contract  
with the U.S. Department of Energy.

Information Services  
Princeton Plasma Physics Laboratory  
P.O. Box 451  
Princeton, NJ 08543

Phone: 609-243-2750  
Fax: 609-243-2751  
e-mail: [pppl\\_info@pppl.gov](mailto:pppl_info@pppl.gov)  
Internet Address: <http://www.pppl.gov>